A&A 529, A83 (2011)
DOI: 10.1051/0004-6361/201116496

Astronomy & Astrophysics

Experimental Stark widths in the Pb IV and Pb V spectra

S. Bukvić, S. Djeniže, Z. Nikolić, and A. Srećković

Faculty of Physics, University of Belgrade, Studentski trg 14, Belgrade, Serbia
e-mail: steva@ff.bg.ac.rs

Received 11 January 2011 / Accepted 23 February 2011

ABSTRACT

Context. The triply and fourthly ionized lead (Pb IV and Pb V, respectively) spectral line shapes have been investigated in the laboratory helium plasma at electron densities ranging between 5.1×10^{22} m^{-3} and 9.1×10^{22} m^{-3} and electron temperatures around 22 000 K (±9%), both interesting for astrophysics.

Aims. The aim of this work is to present experimental Stark *FWHM* (full-width at half of the maximum line intensity, *W*) for 34 spectral lines from Pb IV and 4 spectral lines from Pb V spectra emitted by the pulsed helium discharge, which is optically thin at the wavelengths of the investigated lines. The values presented in this paper are the first published experimental *W* data in the Pb IV and Pb V spectra.

Methods. The lead atoms were sputtered from the cylindrical lead plates that are located in the homogenous part of the pulsed helium discharge at a pressure of 665 Pa in a flowing regime. The Pb IV and Pb V spectral line profiles were recorded using the McPherson model 209 spectrograph and the Andor ICCD camera as the detection system.

Results. The Stark *FWHM*s of 34 Pb IV and 4 Pb V spectral lines were measured in the wavelength interval between 200 nm and 461 nm. Our experimental Pb IV *W* values are compared with the existing theoretical data. Twenty four Pb IV *W* values from the above mentioned set haven't been calculated so far. The isotope shift, caused by the four natural Pb isotopes, and the hyperfine structure have no influence on the observed symmetry of the measured Pb IV and Pb V line shapes at our plasma parameters.

Conclusions. At the mentioned plasma parameters we found a tolerable agreement (within the accuracy of the experiment and uncertainties of the theoretical approaches used) between the measured and calculated ten Pb IV *W* values. For the Pb V spectral lines no comparison is possible because as far as we are aware, no experimental and theoretical *W* data exist.

Key words. plasmas – line: profiles – atomic data

1. Introduction

Lead (Pb, $Z = 82$) belongs to the group of heavy-elements produced by nucleosynthesis processes in the supernovae. Knowledge of its abundance in the stellar atmospheres leads to the better understanding of the production mechanisms of the heavy elements. Recent investigations of lead abundance in various stellar plasmas improve the characterization of the abundance patterns by the *r* (Roederer et al. 2010) and *s* (Bisterzo et al. 2010; Goswami & Aoki 2010) nucleosynthesis processes (of recent examples, only). The triply ionized lead (Pb IV) spectral lines have been identified in various cosmic light sources (Proffitt et al. 2001; O'Toole 2004; Chayer et al. 2006). One can conclude that there is significant interest for the knowledge of the Pb IV spectral lines shape behavior under conditions determined by different plasma parameters. Stark broadening is one of the mechanisms that play an important role in the line shape formation at electron densities (*N*) higher than 10^{22} m^{-3} (Griem 1974). In many models of astrophysical plasmas (Lesage 1994) the Stark width is essential besides the Doppler caused broadening.

The aim of this work is to present the first measured Pb IV and Pb V (four times ionized) Stark *FWHM* (full-width at half of the maximum line intensity, *W*) measured at electron temperature (*T*) ranged around 22 000 K (±9%) and electron density $N = 1 \times 10^{23}$ m^{-3} for the wavelengths above 200 nm.

The Pb IV and Pb V spectra were researched in the helium plasma created by the linear low-pressure pulsed arc. Our experimental Pb IV *W* values are compared with calculated ones (Alonso-Medina et al. 2010). The Pb V Stark widths are not known so far.

Only three works are dedicated to the Pb IV Stark width calculation. Dimitrijević & Sahal-Bréchot (1998, 1999) have calculated *W* values in the Pb IV 6s – 6p and 6s – 7p multiplets in the far vacuum UV region. Alonso-Medina et al. (2010) presented 58 calculated Pb IV *W* values using a semi-empirical approach. For the Pb V lines Stark widths are not calculated or measured so far (NIST 2010; Lesage 2009, and references therein).

Only few experiments (Smith 1930; Crawford et al. 1937; Gutmann 1969, 1973) are devoted to the Pb IV spectrum investigation at wavelengths higher than 200 nm. For the Pb V spectrum only one experiment (Gutmann 1969, 1973) refers to the identified Pb V spectral lines. The tabulated Pb IV and Pb V spectral lines presented by NIST (2010) are taken from Gutmann (1969). The set of papers devoted to the estimation of the Pb IV energy levels with the corresponding quantum transitions is presented by Alonso-Medina et al. (2010).

2. Experiment

A modified version of the linear low-pressure arc (Djeniže 2007, 2009; Bukvić et al. 2009a) was used as a plasma source. A pulsed discharge was created in a glass discharge tube of 5 mm inner diameter with a plasma length of 14 cm (see Fig. 1 in Djeniže 2009). The lead atoms are sputtered from the thin (200 μm) cylindrical lead (99.9% purity) plates located inside the axial part of the discharge tube at its ends. The position

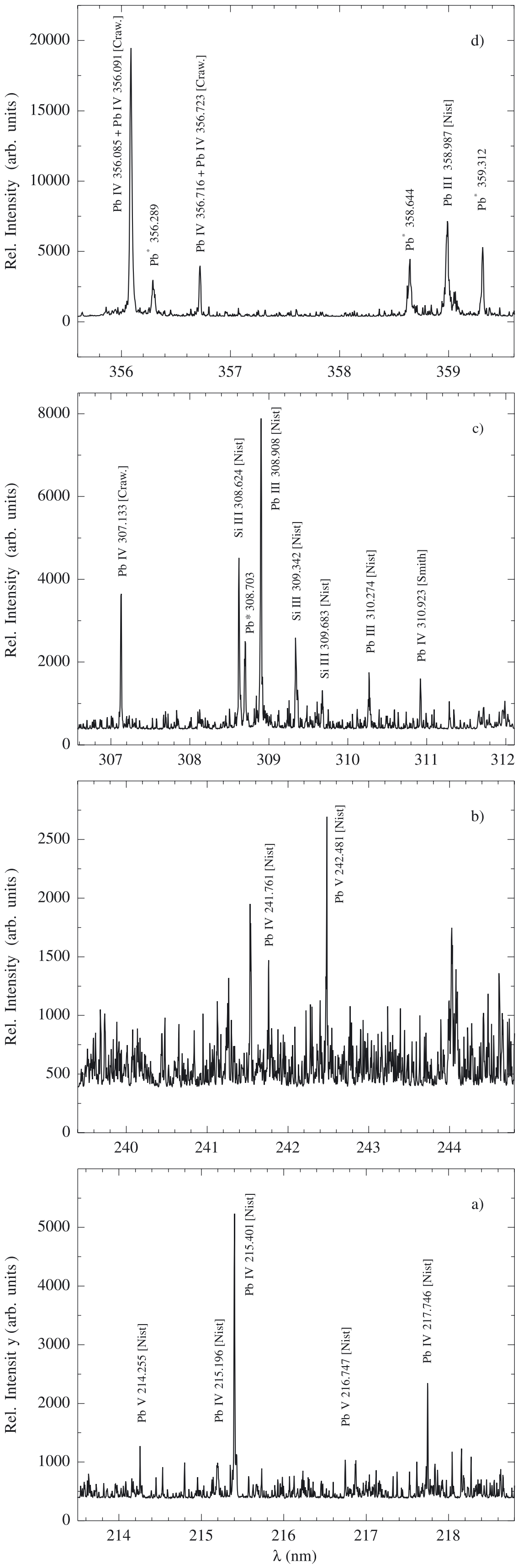

Fig. 1. Panels **a)**–**d)** Profiles of the Pb IV and Pb V spectral lines recorded at various discharge and detection conditions. Asterisks denote values taken from Zaidelj et al. (1977) not classified by ionization stages, while (Craw) is the abbreviation for Crawford et al. (1937) and (Smith) for Smith (1930).

of the plates provides uniform distribution of the sputtered Pb atoms along the optical axis of the homogeneous part of the discharge. The length of the cylindrical plates is 20 mm. The silicon atoms are also sputtered from the glass tube and their spectral lines (Si III and Si IV) can be used for plasma diagnostic purposes. Helium mixture was chosen as the carrier gas (90% He + 7% N_2 + 3% O_2, flowing at 665 Pa pressure). The sputtered lead atoms are efficiently ionized in collisions with helium metastables (triplet with 19.82 eV excitation energy) through the Penning effect (Kruithof & Penning 1937). The final states in this process are the high-lying levels of the singly ionized lead (Pb II). These levels are involved in ionization of Pb II through the electron impact, which results in significant density of excited Pb III ions. Moreover, the ionization of the excited Pb III ions, caused by the collision processes with electrons and He metastables, leads to the density of the Pb IV ions, which ensures intense Pb IV spectral lines.

The discharge is created with the capacitor of 14 μF charged up to 45 J bank energy. Plasma reproducibility was monitored through the radiation originating from the chosen He I, Pb III, and Pb IV lines, and the discharge current with a Rogowski coil signal (Rogowski & Steinhaus 1912). We found that scatter of the peak value of the discharge current is within ±4%.

The McPherson model 209 spectrograph (1.33 m focal length) equipped with 2400 grooves/mm holographic grating, resulting in reciprocal linear dispersion of 0.28 nm/mm in the first order was applied for the spectroscopic observations. As a detection system we employed the Andor DH740-18F-03 iStar intensified CCD camera. The system was calibrated with a set of penlight (Ne, Ar and Hg) sources produced by the LOT-Oriel. We found that the instrumental profile of the spectrograph itself, in the first order measured with 9789 QB EMI photomultiplier, corresponds to the Gaussian function of $FWHM$ = 3.0 pm, while the overall profile (spectrograph + CCD camera) can be approximated by the Voigt function with *FWHM* of 8.7 at 265 nm. Standard light guide and focusing optics, employed at some stages of measurement, have no influence on the shape and width of the instrumental profile.

The spectroscopic observations were made end-on along the axis of the discharge tube. The camera was triggered at the specified moment with an exposure time adapted to our discharge conditions (0.2 μs–0.5 μs). In order to reduce thermal noise, the ICCD detector was always kept at –25 °C. Some of the recorded Pb IV and Pb V spectral line profiles are presented in Fig. 1.

The helium plasma parameters were determined with standard diagnostic methods. Thus, the electron density was estimated relying on the known Stark *FWHM* of the 308.6 nm Si III (Bukvić et al. 2009b) and the He II P_α (468.6 nm) spectral line (Pittman & Fleurier 1986) within ±13% accuracy, connected to the He II P_α *FWHM*. The 308.6 nm Si III line was chosen because it is intense, well isolated (see Fig. 1c), and has a defined profile.

The electron temperature was obtained with the relative line intensity ratio method (Saha equation) (Griem 1964) between Si III (308.62 nm and 309.34 nm) and Si IV (314.96 nm and 316.57 nm) spectral lines with an estimated error of ±14% assuming the existence of the local thermodynamic equilibrium (LTE) (Rompe & Stenbeeck 1967) taking into account the ionization energy lowering (Drawin & Felenbok 1965). The necessary atomic data were taken from NIST (2010). The obtained N and T values ranged between $(5.1–9.1) \times 10^{22}$ m^{-3} and (20 000–23 800) K at the moments when the Stark *FWHM*s are measured.

The absence of self-absorption was checked with a method described by Djeniže & Bukvić (2001). We found that the

Table 1. Measured Pb IV and Pb V Stark widths.

Emitt.	λ^* (nm)	λ^{**} (nm)	Transition	T	W_m	$\frac{W_m}{W_{th}}$
Pb IV	204.258	204.265	$13^{\circ}_{1/2}$–7d $^2D_{3/2}$	2.00 ± 0.28	24.9 ± 5.0	
	204.934	204.937	$24^{\circ}_{7/2}$–5g ^2G	2.00 ± 0.28	49.3 ± 7.4	0.91
	215.196	215.200	6d $^2D_{3/2}$–$25^{\circ}_{1/2}$	2.30 ± 0.32	10.0 ± 2.0	
	215.401	215.401	6p $^2P^{\circ}_{1/2}$–$2_{3/2}$	2.20 ± 0.30	5.0 ± 1.2	
		215.406				
	217.746	217.745	7s $^2S_{1/2}$–$25^{\circ}_{1/2}$	2.30 ± 0.32	5.3 ± 1.6	
	235.953	235.955	$15^{\circ}_{3/2}$–7d $^2D_{5/2}$	2.17 ± 0.30	18.1 ± 2.7	1.13
	241.761	241.77	$15^{\circ}_{3/2}$–7d $^2D_{3/2}$	2.26 ± 0.32	21.5 ± 4.0	
		246.151	$16^{\circ}_{1/2}$–7d $^2D_{3/2}$	2.32 ± 0.32	24.9 ± 3.7	1.13
		249.717	$17^{\circ}_{1/2}$–7d $^2D_{3/2}$	2.23 ± 0.31	10.9 ± 1.9	1.05
		263.774	$18^{\circ}_{5/2}$–7d $^2D_{5/2}$	2.30 ± 0.32	24.2 ± 4.0	
		264.05	$26^{\circ}_{5/2}$–5g $^2G_{7/2}$	2.00 ± 0.28	42.2 ± 6.5	
		273.316	$19^{\circ}_{3/2}$–7d $^2D_{5/2}$	2.00 ± 0.28	67.2 ± 10	
	286.420	286.431	6d $^2D_{3/2}$–$23^{\circ}_{5/2}$	2.38 ± 0.33	49.4 ± 7.4	1.32
	286.450	286.455	6d $^2D_{5/2}$–$24^{\circ}_{7/2}$			
	297.814	297.820	$22^{\circ}_{3/2}$–7d $^2D_{5/2}$	2.30 ± 0.32	36.9 ± 5.5	1.08
		300.276	6d $^2D_{3/2}$–$22_{3/2}$	2.30 ± 0.32	18.5 ± 3.8	
	305.256	305.266	7s $^2S_{1/2}$–$22^{\circ}_{3/2}$	2.22 ± 0.31	25.5 ± 3.8	0.82
		306.243	6d $^2D_{5/2}$–$23^{\circ}_{5/2}$	2.22 ± 0.31	22.5 ± 4.0	
		307.133	$22^{\circ}_{3/2}$–7d $^2D_{3/2}$	2.26 ± 0.32	43.3 ± 6.5	
		314.547	$22^{\circ}_{3/2}$–8s $^2S_{1/2}$	2.10 ± 0.30	39.2 ± 6.0	1.38
	322.117	322.122	6d $^2D_{5/2}$–$22^{\circ}_{3/2}$	2.30 ± 0.32	31.2 ± 4.7	0.72
		356.085	6d $^2D_{5/2}$–$20^{\circ}_{7/2}$	2.18 ± 0.30	25.2 ± 4.0	
		356.091				
		356.716	6d $^2D_{5/2}$–$19^{\circ}_{3/2}$	2.18 ± 0.30	24.5 ± 4.0	
		356.723				
	396.248	396.249	6d $^2D_{3/2}$–$16^{\circ}_{1/2}$	2.26 ± 0.32	47.0 ± 7.0	
	404.980	404.984	7s $^2S_{1/2}$–$16^{\circ}_{1/2}$	2.38 ± 0.33	61.5 ± 9.2	
	449.615	449.625	6d $^2D_{5/2}$–$15^{\circ}_{3/2}$	2.33 ± 0.33	43.5 ± 6.5	
		449.634				
	453.460	453.446	5g $^2G_{9/2}$–6h $^2H^{\circ}$	2.33 ± 0.33	301 ± 24	1.00
		453.493	5g $^2G_{7/2}$–6h $^2H^{\circ}$			
	460.540	460.543	6d $^2D_{5/2}$–$14^{\circ}_{7/2}$	2.33 ± 0.33	53.2 ± 8.0	
		460.553				
Pb V	214.255			2.30 ± 0.32	6.7 ± 1.7	
	216.797			2.15 ± 0.30	7.9 ± 1.6	
	227.666			2.30 ± 0.32	8.3 ± 2.1	
	242.481			2.26 ± 0.32	3.8 ± 1.0	

Notes. Our measured Pb IV and Pb V Stark *FWHM* (W_m in pm with estimated accuracies) at given T (in 10^4 K ±14%) normalized to an $N = 1 \times 10^{23}$ m^{-3}. The symbols $*$ and $**$ denote wavelengths taken from NIST (2010) and Crawford et al. (1937), respectively. W_{th} represents theoretical *FWHM* values presented by Alonso-Medina et al. (2010) except for the four Pb IV wavelengths from Table 2, where the W_{th} denotes the resulting Stark widths (Res. W_{th}) of superposition (see Table 2). Transitions are taken from Crawford et al. (1937) and Gutmann (1969).

intensity ratios of the Pb IV spectral lines are constant (within 14%) during the plasma decay.

The spectral purity of the investigated Pb IV and Pb V lines were checked with a list of the identified wavelengths tabulated by NIST (2010) and Zaidelj et al. (1977).

We suppose that many of the recorded spectral lines belong to the Pb IV and Pb V spectra relaying on the characteristic intensity relaxation (Djeniže 2007). However, at the moment we cannot prove this indication. Thus, we present Stark widths only for already tabulated spectral lines.

3. Line profile deconvolution procedure

The measured Pb IV and Pb V line profiles were of the Voigt type owing to convolution of the Lorentzian Stark, Gaussian profile caused by Doppler, and Voigt instrumental (spectrograph + CCD) broadening. For the electron density and temperature in the experiment presented here, the Lorentzian fraction was dominant. Van der Waals and resonance broadenings (Griem 1974) were estimated to be smaller by more than one order of magnitude than the Stark, Doppler, and instrumental broadenings.

To estimate the spectral line parameters, a deconvolution procedure (Davies & Vaughan 1963) based on the least-squares

Table 2. Superpositions of two Pb IV Lorentz (Stark) profiles.

λ (nm)	Components (nm)	Rel. Int. (a.u.)	Comp. W_{th} (pm)	T (10^4K)	Res. W_{th} (pm)
286.4	286.420	0.75	27.7	2.38	37.3
	286.450	1	35.1	2.38	
246.1	246.151	1	13.4	2.32	22.0
	246.151	1	30.7	2.32	
235.9	235.953	1	14.8	2.17	16.0
	235.953	1	17.5	2.17	
453.4	453.446	1	315	2.33	300.0
	453.493	0.67	275	2.33	

Notes. Superpositions of two Pb IV Lorentz profiles that lie close to each other for four Pb IV lines at a given T and $N = 1 \times 10^{23}$ m^{-3}. Relative intensities (Rel.Int. in arb.units) are taken form Crawford (1937) and the calculated Stark *FWHM* (Comp. W_{th}) are used from Alonso-Medina (2010). The resulting widths (Res. W_{th}) are given in pm.

algorithm was applied. The estimate of the spectrum baseline is based on the procedure presented by Bukvić et al. (2005, 2008).

4. Results and discussion

We have obtained experimental Stark *FWHM*s (W_m) for 34 Pb IV lines. They are presented in Table 1 at the given electron temperature and normalized to an 1×10^{23} m^{-3} electron density. To the knowledge of the authors, these data are the first experimentally obtained results of the Pb IV Stark widths. For ten spectral lines that belong to the investigated set of 34 lines, calculated values (W_{th}) exist. Alonso-Medina et al. (2010) have calculated W values on the basis of a semi-empirical approach using a set of wavefunctions obtained from Hartree-Fock relativistics calculations including core polarization effect. The W_m/W_{th} ratios are presented in Table 1, as well. The W_{th} values are obtained at our temperatures by interpolation (nonlinear B-spline) from Table 1 in Alonso-Medina et al. (2010). Four Pb IV line profiles out of these ten represent superposition of the two closely positioned lines.

Accordingly, we analyzed the effect of the mentioned superposition on the shape of the following spectral lines: 286.4 nm, 246.1 nm, 235.9 nm and 453.4 nm. Wavelengths of the components and their relative intensities are taken from Crawford et al. (1937), while the component Stark widths are used from Alonso-Medina et al. (2010). The resulting profiles are close to the Lorentz profile. We estimated the *FWHM* of the compound distribution numerically in accordance with the definition. Table 2 summarizes our simple analysis. Note that except for the first line in Table 2 (286.4 nm), the width of the composite distribution is less than the width of the broader component. These resulting Stark widths (Res. W_{th}) are, in deed, compared with our W_m values (see Table 1). One can conclude that the W_m and W_{th} values for the 453.4 nm, 235.9 nm and 246.1 nm Pb IV lines (see Table 1) agree very well.

Generally, the difference between W_m and W_{th} values is within ~30% (except for the 314.547 nm line), which can be considered a tolerable agreement with respect to the accuracy of the experiment and the uncertainties of the theoretical approaches used. Our averaged W_m/W_{th} value is higher than 1. It indicates that our W_m values refer to broadening caused by all perturbers. W_{th} (Alonso-Medina et al. 2010) represents broadening realized by electrons as perturbers, only. Additional calculations that include all other possible perturbers (various ions) should be helpful. For the other 24 investigated Pb IV line shapes no theoretical Stark *FWHM* exists. We emphasize that the W_m values of the 215.40 nm, 356.09 nm, 356.72 nm and 449.63 nm Pb IV lines practically correspond to the resulting Stark widths obtained by the superposition of the two closely lying lines (see Table 1 and Figs. 1a, d). The Pb V W_m values are also presented in Table 1.

The observed Pb V lines originate in the high lying, well populated energy levels that are positioned between 39.3 eV and 46 eV excitation energies (Gutmann 1969). Therefore, the Pb V ions in the investigated helium plasma are present at a relatively low electron temperature around 22 000 K, indicating that beside the collision with electrons, many other processes play an important role in the Pb I, Pb II, Pb III, and Pb IV ionization.

Finally, we point out that the isotope shifts, caused by the four natural Pb isotopes (^{204}Pb 1.4%, ^{206}Pb 24.1%, ^{207}Pb 22.1%, and ^{208}Pb 52.4%) and the hyperfine structure (^{207}Pb) have no influence on the observed symmetry of the measured Pb IV and Pb V line shapes at our T and N.

5. Conclusions

Our pulsed helium discharge with the lead cylindrical plates, positioned in the homogeneous part of the discharge, ensures intense and isolated Pb IV and Pb V lines with well defined profiles. Experimental Stark widths of 34 Pb IV and 4 Pb V lines were obtained for wavelengths ranging between 200 nm and 461 nm. The Pb V W_m values are the first data in the Pb V spectrum. Our Pb IV Stark *FWHM* are the first experimental data in the Pb IV spectrum. Ten Pb IV W_m values agree with those calculated on the basis of a semi-empirical approach using a set of wavefunctions obtained from Hartree-Fock relativistics calculations including core polarization effect.

Acknowledgements. This work is part of the "Determination of atomic parameters on the basis of spectral line profiles" (ON171008) project supported by the Ministry of Science and Technological Development of the Republic of Serbia.

References

Alonso-Medina, A., Colón, C., Montero, J. L., & Nation, I. 2010, MNRAS, 401, 1080
Bisterzo, S., Gallino, R., Straniero, O., Cristallo, S., & Käppeler, F. 2010, MNRAS, 404, 1529
Bukvić, S., & Spasojević, D. 2005, Spectrochim. Acta B, 60, 1308
Bukvić, S., Spasojević, D., & Žigman, V. 2008, A&A, 477, 967
Bukvić, S., Djeniže, S., Srećković, A., & Nikolić, Z. 2009a, Phys. Lett. A, 373, 2750
Bukvić, S., Djeniže, S., & Srećković, A. 2009b, A&A, 508, 491
Chayer, P., Fontaine, M., Fontaine, G., Wesemael, F., & Dupuis, J. 2006, Baltic Astron., 15, 131
Crawford, M. F., McLay, A. B., & Crooker, A. M. 1937, Proceed. Roy. Soc. London, Ser. A, 455
Davies, J. T., & Vaughan, J. M. 1963, ApJ, 137, 1302
Dimitrijevic, M. S., & Sahal-Bréchot, S. 1998, Serb. Astron. J., 158, 81
Dimitrijevic, M. S., & Sahal-Bréchot, S. 1999, J. Appl. Spectrosc., 66, 868
Djeniže, S. 2007, Spectrochim. Acta B, 62, 403
Djeniže, S. 2009, Spectrochim. Acta B, 64, 242
Djeniže, S., & Bukvić, S. 2001, A&A, 365, 252
Drawin, H. W., & Felenbok, P. 1965, Data for Plasmas in Local Thermodynamic Equilibrium (Paris, Gauthier-Villars)
Goswami, A., & Aoki, W. 2010, MNRAS, 404, 253
Griem, H. R. 1964, Plasma Spectroscopy (New York: McGraw Hill)

Griem, H. R. 1974, Spectral Line Broadening by Plasmas (New York: Acad. Press)
Gutmann, F. 1969, Spark Spectra of Thallium and Lead, PhD Thesis, The University of British Columbia
Gutmann, F., & Crooker, A. M. 1973, Can. J. Phys., 51, 1823
Kruithof, A. A., & Penning, F. M. 1937, Physica, 4, 430
Lesage, A. 1994, in Astrophysical Applications of Powerful New Databases, ed. S. J., Adelman, & W. L. Wiese, ASP Conf. Ser., 78
Lesage, A. 2009, New Astron. Rev., 52, 471
NIST 2010, Atomic Spectra Database Lines (wavelength order), http://www.physics.nist.gov
O'Toole, S. J. 2004, A&A, 423, L25
Pittman, T. L., & Fleurier, C. 1986, Phys. Rev. A, 33, 1291
Proffitt, C. R., Sansonetti, C., & Reader, J. 2001, ApJ, 557, 320
Roederer, I. U., Cowan, J. J., Karakas, A. I., et al. 2010, ApJ, 724, 975
Rogowski, W., & Steinhaus, W. 1912, Archiv für Elektrotechnik, 1, 141
Rompe, R., & Stenbeeck, M. 1967, Ergebnisse der Plasmaphysik und der Gaselektronik (Berlin: Akademie Verlag)
Smith, S. 1930, Phys. Rev., 36, 1
Zaidelj, A. N., Prokofjev, V. K., Raijskij, S. M., Slavnjij, V. A., & Shrejder, E. Y. 1977, Spectral Line Tables (in Russian) (Moscow, Nauka)